Title
Comparison of steady-state and perturbative transport coefficients in TFTR

Journal
Physics of Plasmas, 3(8)

ISSN
1070-664X

Authors
Efthimion, PC
Barnes, CW
Bell, MG
et al.

Publication Date
1991-08-01

DOI
10.1063/1.859598

Comparison of steady-state and perturbative transport coefficients in TFTR

P. C. Efthimion, C. W. Barnes, M. G. Bell, H. Biglari, N. Bretz, P. H. Diamond, G. Hammett, W. Heidbrink, R. Hulse, D. Johnson, Y. Kusama, D. Mansfield, S. S. Medley, R. Nazikian, H. Park, A. Ramsey, G. Rewoldt, S. D. Scott, B. C. Stratton, E. Synakowski, W. M. Tang, G. Taylor, M. C. Zarnstorff, and S. J. Zweben

Citation: Physics of Fluids B: Plasma Physics **3**, 2315 (1991);

View online: https://doi.org/10.1063/1.859598

View Table of Contents: http://aip.scitation.org/toc/pfb/3/8

Published by the American Institute of Physics

Comparison of steady-state and perturbative transport coefficients in TFTR*

P. C. Efthimion,† C. W. Barnes,[a] M. G. Bell, H. Biglari, N. Bretz,
P. H. Diamond,[b] G. Hammett, W. Heidbrink,[c] R. Hulse, D. Johnson, Y. Kusama,[d]
D. Mansfield, S. S. Medley, R. Nazikian, H. Park, A. Ramsey, G. Rewoldt, S. D. Scott,
B. C. Stratton, E. Synakowski, W. M. Tang, G. Taylor, M. C. Zarnstorff,
and S. J. Zweben
Plasma Physics Laboratory, Princeton University, P.O. Box 451, Princeton, New Jersey 08543

(Received 9 January 1991; accepted 24 April 1991)

Steady-state and perturbative transport analysis are complementary techniques for the study of transport in tokamaks. These techniques are applied to the investigation of auxiliary-heated L-mode and supershot plasmas in the tokamak fusion test reactor (TFTR) [R. J. Hawryluk *et al.*, *Plasma Physics and Controlled Nuclear Fusion Research*, Proceedings of the 11th International Conference, Kyoto, 1986 (IAEA, Vienna, 1987), Vol. 1, p. 51.]. In the L mode, both steady-state and perturbative transport measurements reveal a strong temperature dependence that is consistent with electrostatic microinstability theory and the degradation of confinement with neutral beam power. Steady-state analysis of the ion heat and momentum balance in supershots indicates a reduction and a significant weakening of the power-law dependence on the transport in the center of the discharge.

I. INTRODUCTION

Steady-state heat and momentum balance analysis is universally applied to the study of transport in tokamak plasmas. Perturbation analysis has also become a popular means of obtaining additional information about transport.[1-7] These techniques are complementary, and together they offer a powerful means of studying transport in tokamaks. The research program on TFTR has focused upon understanding transport in its auxiliary-heated plasma regimes: the L mode and supershots. The L-mode regime has been studied on every tokamak with auxiliary heating.[8-12] Unfavorable confinement scaling with heating power ($\tau_E \propto P^{-0.5}$) makes the L mode unattractive as a reactor regime. Understanding the cause of the adverse power dependence in the global confinement time is important, and reactor-relevant because it is also observed in the H modes. Supershots have enhanced confinement compared to L-mode, $\tau_E/\tau_E^{L\ \mathrm{mode}} \sim 2$–3, peaked pressure profiles, high temperatures, and the absence of confinement degradation with input power until the β limit is reached making them relevant to reactor studies.[13] In this paper, the TFTR confinement in auxiliary-heated plasmas obtained from perturbative and steady-state transport analysis are compared.

The relative advantages and disadvantages of steady-state and perturbative transport analysis can be illustrated by examining the particle continuity equation

$$\frac{\partial n}{\partial t} = -\nabla\cdot\Gamma + S, \tag{1}$$

where one model for the particle flux Γ is $\Gamma = -D\nabla n + Vn$, D is the particle diffusivity, V is the radial velocity, S is the particle source, and n is the density. A steady-state solution for Γ requires an accurate determination of the particle source term. In contrast, a perturbative solution of the particle continuity equation relies on variations of the density and the particle source terms instead of the absolute value of the terms. In the case of a perturbation by a gas puff, $\partial n/\partial t$ dominates the source in Eq. (1). Furthermore, in steady state, the decoupling of Γ into transport coefficients D and V is impossible because there is only one equation and two unknowns; only the ratio D/V is obtainable. Perturbative techniques take advantage of the time variation of the data to produce a system of equations with more equations than unknown transport coefficients. It is important that the system of equations is not degenerate when there is more than one unknown. This is satisfied if the terms multiplying the transport coefficients are decorrelated in time. For example, a perturbation in the form of a small gas puff decouples the perturbed density and density gradient, δn and $\delta\nabla n$, due to their different time behaviors. This enables the transport coefficients to be determined from the perturbed flux.

A disadvantage of perturbation analysis is that the perturbation must be small to minimize the deviation from steady-state conditions. Thus, many reproducible shots may be required to obtain good measurement accuracy. This can be a problem in some auxiliary-heated plasmas where irreproducible shot-to-shot variations can be as large as the perturbation. More important, there are fundamental issues in perturbation analysis that are not always understood: the steady-state parameters are not always measured and nonlinear dynamics [i.e., $D = D(n, \nabla n)$] complicates the analy-

*Paper 1I02, Bull. Am. Phys. Soc. **35**, 1917 (1990).
†Invited speaker.
[a] Permanent address: Los Alamos National Laboratory, Los Alamos, New Mexico 87545.
[b] Permanent address: University of California, San Diego, La Jolla, California 92093-0319.
[c] Permanent address: University of California, Irvine, Irvine, California 92717.
[d] Permanent address: Naka Fusion Research Establishment, JAERI.

 0899-8221/91/082315-09$02.00

sis. These two points are illustrated in the linearized perturbed particle flux equation with nonconstant transport coefficients

$$\delta\Gamma = \left(-\langle D\rangle - \frac{\partial D}{\partial \nabla n}\langle \nabla n\rangle + \frac{\partial V}{\partial \nabla n}\langle n\rangle \right)\delta\nabla n + \left(\langle V\rangle + \frac{\partial V}{\partial n}\langle n\rangle - \frac{\partial D}{\partial n}\langle \nabla n\rangle \right)\delta n, \quad (2)$$

where $\langle\ \rangle$ and δ represent the steady-state and perturbed quantities, respectively. A serious problem arises in the terms multiplying δn because the particle diffusivity contributes to the apparent pinch. The pinch commonly refers to the velocity terms multiplying δn in $\delta\Gamma$. If D is proportional to L_n^{α}, the nonlinear term, $\partial D/\partial n\,\langle \nabla n\rangle$, will be larger than the neoclassical pinch velocity. Neglecting the nonlinear diffusivity term could lead to the erroneous conclusion that the pinch is highly anomalous. The terms multiplying $\delta\nabla n$ include the steady-state diffusivity $\langle D\rangle$ and a nonlinear term, $\partial D/\partial\nabla n\,\langle\nabla n\rangle$. Note this term is of the same order as $\langle D\rangle$ if D is proportional to L_n^{α} and $\alpha \neq 0$. Similar issues concerning the advantages and disadvantages of steady-state and perturbative thermal transport analysis can be inferred from the heat balance equation.

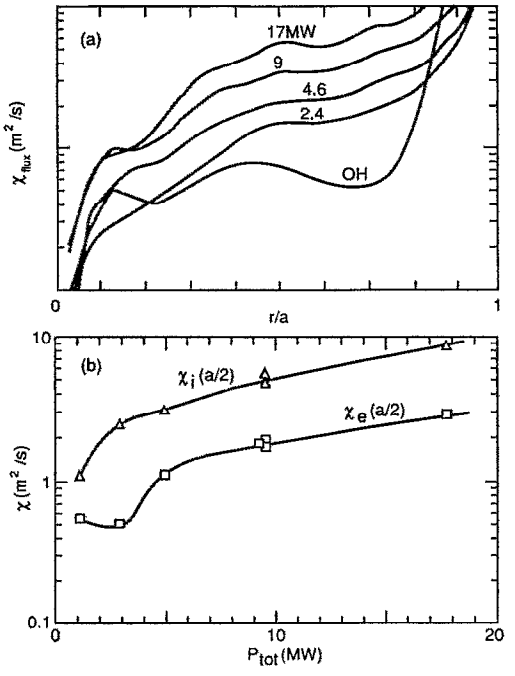

FIG. 1. (a) The single-fluid χ_{flux} radial profile for an L-mode neutral beam power scan. (b) The electron and ion heat diffusivity at $r/a = 0.5$ for the L-mode neutral beam power scan.

II. L-MODE PLASMAS

A. Steady-state transport

Steady-state L-mode plasma transport was studied in a power scan at constant density, where the central density $n_e(0) = 4\times 10^{19}\ \mathrm{m}^{-3}$, the plasma current $I_p = 1.2$ MA, the major radius R = 2.58 m, the minor radius $a = 0.93$ m, and the toroidal magnetic field $B\varphi = 3.8$ T.[14] Local coefficients of energy transport were determined from profile measurements of temperature, density, and radiation using the 1-D steady-state transport analysis code SNAP.[15] Figure 1 illustrates the radial dependence of the single-fluid thermal diffusivity, $\chi_{flux} \equiv -(Q_e + Q_i)/(n_e\nabla T_e + n_i\nabla T_i)$, where Q_e and Q_i are the electron and ion heat fluxes and ∇T_e and ∇T_i are the electron and ion temperature gradients, for several values of auxiliary power. Here, χ_{flux} characterizes the average thermal heat transport and avoids difficulties in L-mode plasmas of separating the total heat flow into convective and conductive channels and ion and electron channels. (Classical electron–ion heat exchange can be a very large term in the power balance in the outer part of the plasma where the temperatures are low. Moreover, possible anomalous contributions to this exchange are not considered.) The value χ_{flux} increases with input power at all radii while keeping its profile shape relatively constant. In Fig. 1(b), the heat fluxes for electrons and ions are separated and their corresponding thermal diffusivities are shown at half the minor radius. In the L mode, the ions dominate the power flow, χ_i is greater than χ_e, and both increase strongly with beam power. Magnetic measurements of the stored energy for L-mode plasmas, including the well-confined fast ions, imply that the total energy confinement τ_E scales as $\tau_E \propto P_b^{-0.5}$, where P_b is the neutral beam heating power.[8] By contrast, kinetic measurements not including the fast-ion stored energy indicate a stronger power-law dependence for the thermal confinement[14,16] $\tau_{thermal}$ described as $\tau_{thermal} \propto P_b^{-0.7}$.

B. Perturbative electron transport

Perturbative analysis has been applied to the study of particle transport in L-mode plasmas.[17] The electron particle transport coefficients are ascertained by measuring $n_e(r,t)$ following a small gas puff that perturbs the line-integrated density $\int\delta n_e\,dl/\int n_e\,dl \sim 7\%$. The flux $\Gamma(r,t)$ is obtained from Eq. (1) using the density profile measured from a ten-channel interferometer and the electron particle source. The dominant electron source comes from the steady-state neutral beam fueling, and the wall electron source is calculated using an estimate for the edge particle confinement time based upon measurements of H_α radiation in the limiter region.

Because of the potential problem with nonconstant transport coefficients, a general linearized form of the perturbed particle flux is used:

$$\delta\Gamma = \frac{\partial\Gamma}{\partial\nabla n}\delta\nabla n + \frac{\partial\Gamma}{\partial n}\delta n, \quad (3)$$

where the partial derivatives will now be referred to as the transport coefficients.

This approach was applied to L-mode plasmas to ascertain the temperature dependence of transport. The motivation for this study comes from the theory of anomalous transport due to microinstabilities. A few analytic forms of the theory[18-20] are

$$D_{dte} = \epsilon^{1.5}(\rho_s C_s/L_n)^2/\nu_{ei} \propto \epsilon^{1.5}T_e^{3.5}/(nL_n^2), \quad \nu_{eff}/\omega^* \gg 1, \quad (4)$$

$$D_{\rm cte} = 3\epsilon^{0.5}\rho_s C_s^2/L_n \propto \epsilon^{0.5}T_e^{1.5}/L_n, \quad \nu_{\rm eff}/\omega^* \ll 1, \tag{5}$$

$$D_{\rm itg} = \epsilon^{0.5}(\rho_s C_s)^2 L_s/(\nu_{\rm eff} L_{Ti}{}^3) \propto \epsilon^{0.5}T_e^{3.5}L_s/L_{Ti}^3, \tag{6}$$

where $D_{\rm dte}$ and $D_{\rm cte}$ are estimates of the diffusivities for the dissipative and collisionless trapped-electron mode and $D_{\rm itg}$ represents a sheared-slab model estimate of the diffusivity for the trapped-ion mode in the dissipative trapped-electron regime of collisionality. Here, ρ_s is the ion Larmor radius evaluated using the electron temperature, C_s is the sound speed, L_n, L_{Ti}, and L_s are the density gradient, ion-temperature gradient, and shear scale lengths, T_e is the electron temperature, n is the electron density, ν_{ei} is the electron–ion collision frequency, $\nu_{\rm eff} = \nu_{ei}/\epsilon$, ϵ is the inverse aspect ratio, and ω^* is the diamagnetic drift frequency. These analytic forms of $D_{\rm dte}$ and $D_{\rm cte}$ are strictly applicable only at the two extreme limits of collisionality. In many plasmas, including those with L-mode confinement, $\nu_{\rm eff}/\omega^* \approx 1$. A recent model[21] for trapped-electron transport in this regime of collisionality indicates that the T_e and L_n dependencies are functions of $\nu_{\rm eff}/\omega^*$ and L_n.

The dependence of the local particle and heat transport coefficients on temperature were measured during a neutral beam power scan, with the final density during beam injection held constant. Four beam powers were used with the power in the co- and counter-beam sources balanced to minimize plasma rotation ($P_b = 0$, 4.5, 9.0, and 14 MW). The other constant plasma parameters were toroidal magnetic field $B\varphi = 4.0$ T, major radius $R = 2.58$ m, minor radius $a = 0.93$ m, safety factor $q = 5.1$, and the plasma current $I_p = 1.5$ MA. The gas puff was produced with a flow rate of 15 torr-liters/sec for 0.05 sec in the steady-state period of the neutral beam injection. Figure 2 shows the four electron density and temperature profiles from the scan. The central electron temperature varied by a factor of two while the density profiles were successfully held constant. There is similar ion heating with the ratio of T_i/T_e increasing from 0.8 to 1.25 with input power. The global energy confinement time for plasmas in increasing order of input power were 0.27, 0.127, 0.105, and 0.100 sec. The confinement times were, on the average, 1.1 times L-mode confinement scaling.[8]

The general flux analysis [Eq. (3)] is applied outside the $q = 1$ ($q = 1$ at $r = 0.23$ m) surface to avoid density sawtooth effects, but not within 0.23 m of the last closed flux surface of the tokamak in order to minimize the influence of the edge electron source term in the particle balance and the radiative power term in the heat balance. Figures 3(a) and 3(b) show the particle transport coefficients, $\partial\Gamma/\partial\nabla n$ and $\partial\Gamma/\partial n$, derived from the flux analysis as a function of radius for the four plasma cases described in Fig. 2. At each radius, there is an increase in the particle transport coefficients with increasing temperature. There is also a radial dependence in the coefficients with smaller values toward the center of the plasma. The electron and ion thermal conductivities, χ_e and χ_i [Fig. 3(c)] obtained from equilibrium power balance analysis exhibit similar temperature behavior to $\partial\Gamma/\partial\nabla n$ [Fig. 3(a)]. These L-mode plasmas, as well as those in Sec. II A have $\chi_i > \chi_e$.

At each radius, the transport coefficients in Fig. 3 are assumed to be proportional to T_e^α, and the temperature exponent is plotted in Fig. 4 as a function of radius. Note that $\partial\Gamma/\partial\nabla n$ and $\partial\Gamma/\partial n$ exhibit the same temperature scaling at each radius, with temperature exponents ranging from 1.5–2.5. Similar values of temperature exponent are obtained for χ_e and χ_i. The temperature dependence of the single-fluid thermal diffusivity $\chi_{\rm flux}$ at each radius for the neutral beam-heated plasmas is also shown in Fig. 4, and is similar to the values obtained for the particle transport coefficients $\partial\Gamma/\partial\nabla n$ and $\partial\Gamma/\partial n$.

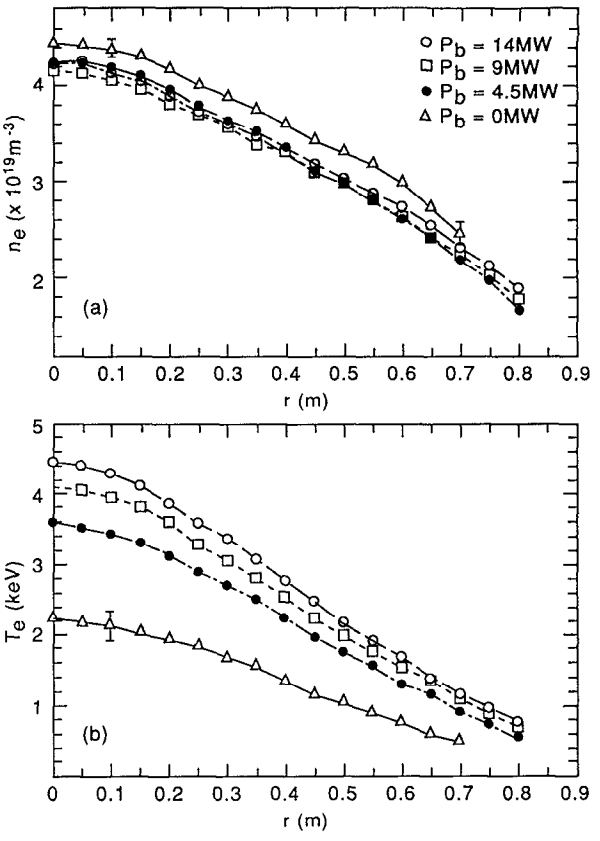

FIG. 2. The electron density and temperature profiles at four neutral beam powers (0, 4.5, 9.0, 14 MW).

The temperature exponents observed for the heat and particle transport coefficients are between the values of 1.5 and 3.5 predicted by the analytic forms of trapped-particle drift-type microinstability transport theory for the two extremes of collisionality in the banana regime. With $\nu_{\rm eff}/\omega^* \approx 1$, Waltz and Dominguez[21] indicate that the temperature exponent should lie between 1.5 and 3.5. More accurate values are obtained from two numerical codes that calculate the temperature exponent from microinstability theory. The first is a comprehensive kinetic quasilinear microinstability calculation in toroidal geometry for trapped-particle modes driven by trapped-electron and ∇T_i [$\eta_i \equiv \partial(\ln T_i)/\partial(\ln n_i)$] dynamics (referred to as the toroidal QL model).[22] For $r < 0.65$ m, $\eta_i > 2$, this calculation indicates that η_i mode behavior should be dominant. Anomalous transport coefficients were estimated using quasilinear theory, with fluctuation levels evaluated using the mixing length prescription $e\varphi/T_e \equiv 1/k_\theta L_p$, where k_θ is the poloidal wave vector and L_p is the pressure gradient scale

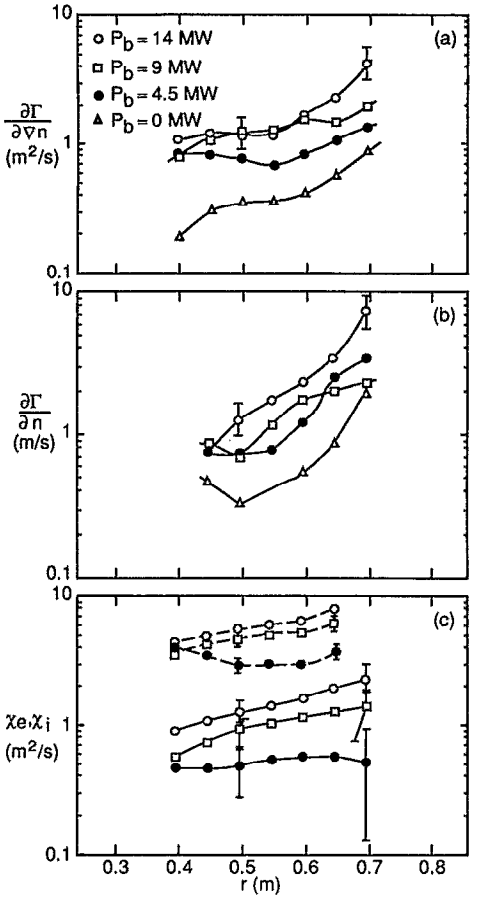

FIG. 3. (a) Particle transport coefficient $\partial\Gamma/\partial\nabla n$ versus plasma radius at four neutral beam powers (0, 4.5, 9.0, 14 MW). (b) Particle transport coefficient $\partial\Gamma/\partial n$ versus plasma radius at four neutral beam powers (0, 4.5, 9.0, 14 MW). (c) Electron and ion thermal diffusivities (χ_e, χ_i) versus plasma radius. The points with dashed lines are χ_i and those with solid lines are χ_e.

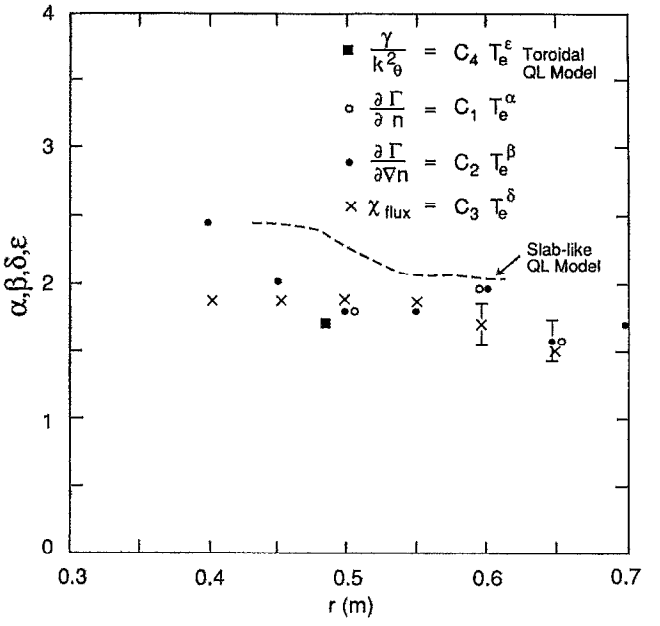

FIG. 4. The electron temperature exponent of the transport coefficients $\partial\Gamma/\partial\nabla n$, $\partial\Gamma/\partial n$, and χ_{flux}, and a comparison with the exponents from two drift-like microinstability models (slab-like QL model, and toroidal QL model).

length. Note that, for toroidal modes, $k_r \approx k_\theta \hat{s}\Delta\theta$, where $\Delta\theta$ is the extent of the wave along a magnetic field line. The second calculation[21] is a slab-like quasilinear model of trapped-particle transport (referred to as slab-like QL model) assuming that the η_i mode behavior is dominant. For the toroidal QL model, the average of the temperature exponents (i.e., $D \propto T^{\beta}$) of the particle (and electron thermal) diffusivity at $r = 0.5$ m for the four cases is shown in Fig. 4. The average of the calculated exponents is very close to the experimentally deduced exponent of the particle (and electron thermal) diffusivity at the same radius. Furthermore, the calculated ratio of the ion and electron heat fluxes, Q_i/Q_e, is 3.1, which is within 50% of the value obtained from the steady-state heat balance. For the slab-like QL model, the average temperature exponents over the radii $r = 0.35$–0.6 m are shown as a dotted line in Fig. 4, and are also close to the experimental results. Because the neutral beam deposition does not change in the power scans at constant density, the roughly temperature-squared dependence in χ_{flux} is easily related to a global thermal confinement power dependence of $\tau_{thermal} \propto P_b^{-0.66}$. This is in agreement with the power-law dependence in the steady-state analysis for the thermal particles (Sec. II A). While the calculations have focused on η_i modes, these results are consistent with the temperature scaling of generic drift-like microinstabilities.

Although these experiments have shown that the temperature dependence of the local particle and heat transport is consistent with electrostatic theory, they have not uniquely determined the scale length dependence of the transport coefficients. Also, it is important to acknowledge that we have not reconciled here the differing radial dependence of the measured transport coefficients, which increase with radius, with the theory-based coefficients, which decrease with radius because of the temperature dependence. In a future publication, it will be shown that the radial dependence of the particle transport coefficients can be reconciled with the temperature and density scale lengths.

C. Microwave scattering

A spatially scanning microwave scattering system operating in the extraordinary mode at 60 GHz is used to study small-scale density fluctuations in TFTR plasmas.[23] Heterodyne measurements of density fluctuations are made in the wave-number range $2.0\ \text{cm}^{-1} < k_\perp < 25\ \text{cm}^{-1}$. Spatial resolution determines the low $k_\perp$ limit at $2.0\ \text{cm}^{-1}$. The spectral power density integrated over frequency S_k at $r \approx 0.3$ m for linear Ohmic and L-mode plasmas have their highest fluctuation amplitudes occuring at the longest resolvable scale lengths corresponding to $k_\perp \rho_s < 0.5$, where ρ_s is the ion Larmor radius calculated with the electron temperature. The change in spectra from Ohmic to L mode was examined for the same set of discharges used in Fig. 1, where the density was kept constant in a neutral beam power scan [Fig. 5(a)]. The spectrum for the L mode with 9 MW of beam power has a higher amplitude and is more peaked at low k, leading to an

increase in $\delta n_e/n_e$ by a factor of 3.3 between Ohmic and L mode. The magnitude of the density fluctuations can be fitted with a power law of $S_k \propto 1/k_\perp^3$ for the L-mode plasma, and $S_k \propto 1/k_\perp^2$ for the Ohmic plasma. At fixed $k_\perp = 4.2$ cm^{-1}, with the density held constant, the scattered power increases with total heating power and is plotted in Fig. 5(b) versus electron temperature. The single-fluid thermal diffusivity χ_{flux} shown in Fig. 1 is plotted for $r \approx 0.3$ m in Fig. 5(b). The thermal diffusivity and the scattered spectrum at $k_\perp = 4.2$ cm^{-1} roughly correlate with electron temperature. This comparison was made with L-mode discharges with beam power $\leqslant 9$ MW and Ohmic discharges. In Fig. 5(b), S_k and χ_{flux} can be expressed as an electron temperature power law with exponent near 2, and an exponent of 2.8 if the Ohmic points are not included. From scattering theory, $\delta n_e^2 \propto \int S_k \, d\mathbf{k}$, where $d\mathbf{k}$ is the wave-vector differential element. Note that $\delta n_e^2 \propto \chi_{\text{flux}}$ from Fig. 5(b) and $\chi_{\text{flux}} \propto T^\beta$, where $\beta \sim 2$ from the experiments in the previous section. Electrostatic theory expects the temperature dependence of δn_e^2 and χ_{flux} to differ by $T_e^{1/2}$, but the accuracy of the measurements and the limited data points do not allow for such differences to be resolved. Nonetheless, these observations are consistent with the turbulence causing the transport, as expected from electrostatic microinstability theory.

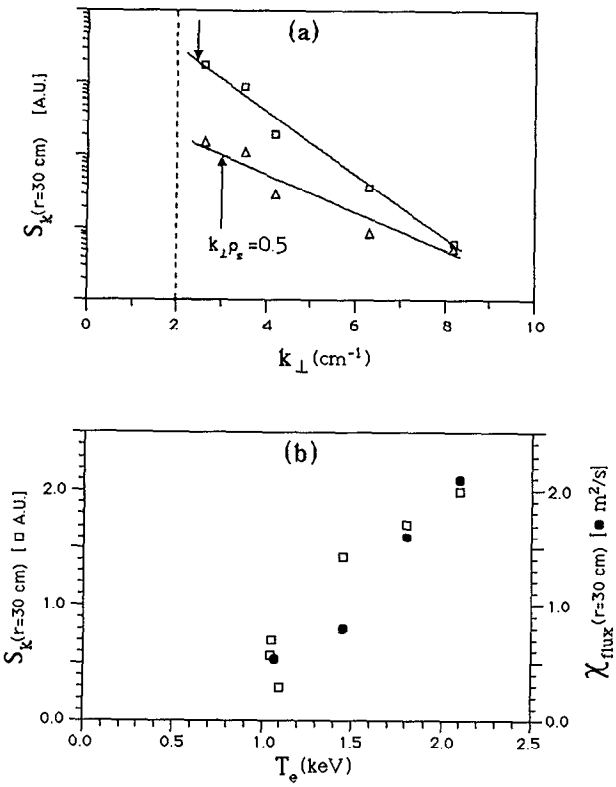

FIG. 5. (a) The relative magnitude of the density fluctuations, $S_k \propto \langle \delta n_e^2 \rangle$, versus $k_\perp$ from microwave scattering is shown for Ohmic and 9.1 MW L-mode discharge. (b) The relative magnitude of the density fluctuations, $S_k \propto \langle \delta n_e^2 \rangle$, at $r = 0.3$ m and $k_\perp = 4.2$ cm^{-1}; and the single-fluid heat diffusivity χ_{flux} at the same radius versus electron temperature.

D. Trace He^{+2} transport

A powerful perturbation technique is based on measurement of the radial profile of the He^{+2} transport coefficient using charge-exchange spectroscopy after the introduction of a small helium gas puff into a deuterium plasma.[24] The technique was applied to high-recycling plasmas at $I_p = 1.4$ MA with confinement slightly higher than L mode. Neutral beam power of 6.7 MW was injected coparallel to the plasma current for 1.0 sec; as a result, these discharges exhibit toroidal rotation with a central velocity of 250 km/sec. The measured time evolution of the helium density at several radii in the plasma has been modeled with the impurity transport code MIST.[25] This permits determination of transport coefficients as a function of radius. The best fit to the time history of the helium density perturbation at different radii requires a particle diffusivity that increases with radius (Fig. 6); a spatially constant diffusivity will not reproduce the data. Across the entire plasma cross section, both the measured diffusivity and convective velocity are at least an order of magnitude larger than values predicted by neoclassical theory. The inward convective velocity is approximately 8 m/sec at $r = 0.6$ m and 35 m/sec at the plasma edge. The helium particle diffusivity has been compared to thermal and momentum diffusivities calculated with the 1-D steady-state transport code SNAP. The ion, electron, and momentum diffusivities, χ_i, χ_e, and χ_φ, are shown in Fig. 6 for a comparison with the helium diffusivity. It is clear that $D_{\text{He}}(r) \sim \chi_i(r) \sim \chi_\varphi(r) > \chi_e(r)$ over the plasma cross section in this L-mode plasma. This result may be consistent with plasma transport because of electrostatic microinstabilities. Numerical calculations of the ratio of the ion and electron heat flux as a function of the parameter $\eta_i \equiv \partial(\ln T_i)/\partial(\ln n_i)$ show $\chi_i(r) \sim \chi_\varphi(r) > \chi_e(r)$ when $\eta_i > 1$.[22] In this regime, the perturbed ion pressure can be out of phase with the perturbed electrostatic potential. If the helium is considered a trace impurity, ambipolarity does not govern its transport and the helium ions may then transport at a rate comparable to that of ion heat transport, i.e., $D_{\text{He}}(r) \approx \chi_i(r)$.

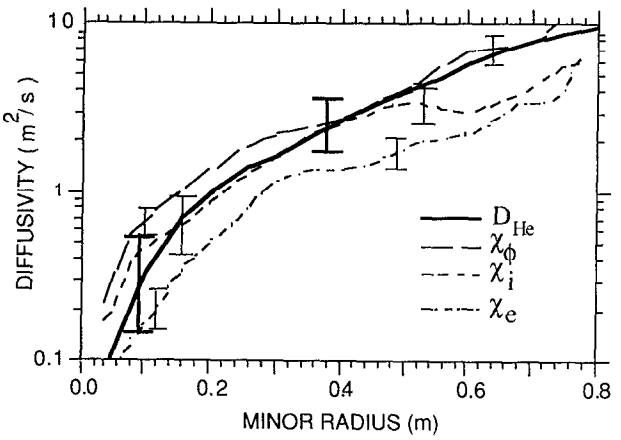

FIG. 6. Helium diffusivity $D_{\text{He}}(r)$, electron thermal diffusivity χ_e, ion thermal diffusivity χ_i, and momentum diffusivity χ_φ as calculated with SNAP.

E. Trace iron transport

Transport of a trace amount of iron injected into the same L-mode plasmas used to study helium transport was measured with the CHERS diagnostic.[26] The diffusivity of helium-like iron (Fe^{24+}), the most abundant iron ion in the core of these discharges, is flatter than the helium diffusivity, increasing from 1.3 m^2/sec on axis to 2.4 m^2/sec at the plasma edge. These values are larger by over an order of magnitude than the neoclassical diffusivity, while the measured convective velocity, which rises from 0 on axis to 6 m/sec at the edge, is consistent with the neoclassical values. Modeling is underway to see whether the observed difference between helium and iron transport can be explained by electrostatic turbulence; the effects of plasma rotation may also be important.

III. SUPERSHOT PLASMAS

A. Steady-state transport

The supershot is an enhanced confinement plasma with $\tau_e/\tau_e^{\text{L mode}} \sim 2$–$3$.[13,27–29] Supershots are characterized by peaked density profiles [$n_e(0)/\langle n_e\rangle \leqslant 3$], high ion temperatures ($T_i \sim 20$–30 keV), and are formed by core fueling a low-recycling, low-density target plasma with balanced neutral beam injection. The steady-state transport properties of the low-recycling and high-recycling plasmas have been compared in a pair of neutral beam power scans at $I_p = 1.3$ MA and beam powers between 5 and 23 MW.[14] The neutral beam injection was unbalanced to allow for measurement of the momentum diffusivity with a constant torque during the neutral beam power scans. At low power, the unbalanced injection was coinjected only and $n_e(0)/\langle n_e\rangle \sim 2.1$, while the high-power end is a mix of co- and counter-injection and $n_e(0)/\langle n_e\rangle \sim 2.4$. Unbalanced injection in a low-recycling target plasma does not result in the high-peaked density profiles characteristic of supershots, nevertheless, these plasmas did have enhanced confinement compared to L-mode plasmas ($\tau_E/\tau_E^{\text{L mode}} \leqslant 2.6$ at the high beam powers) and high ion temperatures. The high-recycling plasmas did have L-mode characteristics. The characteristics of the two plasmas are compared in Fig. 7. The supershot label is in quotes because the data points below 10 MW have only modestly peaked density profiles; this regime is usually referred to as "the hot-ion mode".[30] The line average density in supershots increases with beam power, while the high-recycling L mode shows little density variation despite the substantial increase in the particle fueling rate during the neutral beam power scan. The central electron temperature increases with power in both cases although the supershot is at least 50% hotter. A striking difference between the two plasma regimes is that the ion temperature is a factor of 2–3 larger in the supershots than in the L-mode plasmas.

The angular momentum plays an analogous role in the momentum balance to the stored energy in the energy balance. Note the interesting trend that the central angular momentum density, shown in Fig. 7, increases with power in the supershot plasma and decreases in the L-mode plasmas, *at fixed torque input*. This is direct evidence for degradation of momentum confinement with beam power for the L mode, and improvement in the case of the supershot. The local power balance shows an improvement in χ_i at all radii in the supershot (Fig. 8). Although the improvement in χ_i is marginally better in the plasma core compared to the half-radius, the power-law dependence in χ_i in the core has been significantly weakened. A stronger case can be made for χ_φ, which has smaller error bars than χ_i. For χ_φ, the improvement in the supershot is primarily in the plasma core. The unfavorable power dependence for the momentum transport is actually reversed in the core of the supershot. Confinement trends between L-mode and supershot plasmas have been correlated with the density profile peakedness, $n_e(0)/\langle n_e\rangle$.[28] This correlation could either be caused by a favorable effect of peakedness on confinement, or is the result of improved particle confinement caused by some other change. It is important to note that $T_i/T_e > 2$ for supershots and may be a factor in determining the improvement in the transport. At the higher-input powers, the density peakedness (Fig. 8) increases in supershots and decreases in the L mode.

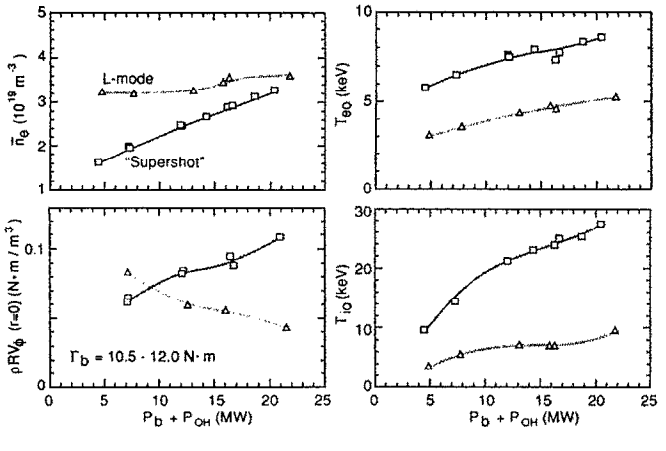

FIG. 7. Comparison of the characteristics of L-mode and "supershot" plasmas in a constant torque neutral beam power scan.

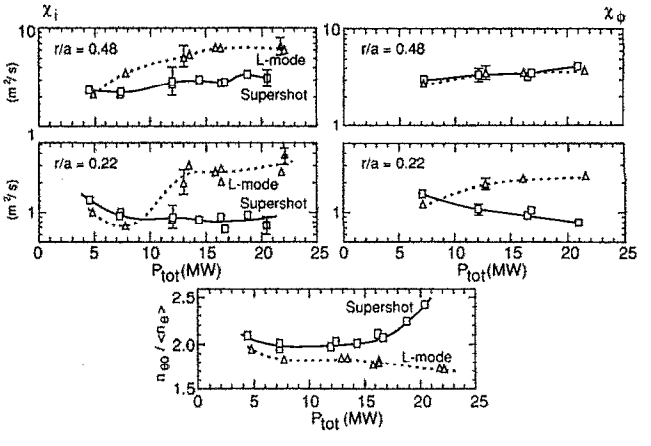

FIG. 8. Comparison of χ_i, χ_φ, and $n_e(0)/\langle n_e\rangle$ for the L-mode and "supershot" plasmas in a constant torque neutral beam power scan.

B. Perturbative studies of marginal stability

As shown in Sec. II A, steady-state supershot transport studies indicate a correlation between a reduction in the thermal and momentum diffusivities and increased peakedness of the density profile. The ion temperature and density profiles shapes are similar, with the result that the supershot plasmas are predicted to be near marginal stability for ion temperature gradient driven turbulence (ITGDT). If the predicted transport due to ITGDT is much greater than the steady-state transport, the turbulence would be expected to enforce marginal stability. Marginal stability in supershots was tested by transiently broadening the peaked density profiles with injection of either pellets or a helium gas puff.[30,31] Marginal stability to ITGDT would result in the thermal ion transport adjusting the temperature profile to the shape of the density profile in order to return the threshold parameter $\eta_i \equiv \partial(\ln T_i)/\partial(\ln n_i)$ to a value near the threshold η_c. The supershot plasmas tested have $I_p = 1.0$ MA, $B_\varphi = 4.8$ T, $R = 2.45$ m, and 14 MW of balanced neutral beam injection. The helium puff perturbed the outer half of the plasma while the pellet perturbation modified most of the profile. For both perturbations, the plasmas are driven far from the theoretical stability boundary for ITGDT. At $r/a = 0.67$, η_i is near 2 before the perturbation and reaches a peak value near 9, and remains above 5 for more than 0.035 sec. However, the threshold values of η_c predicted by Romanelli,[32] Hahm and Tang,[33] and Mattor and Diamond[34] reach peak levels of 3, 4, and 4.5, respectively, in the condition of this experiment. Although the density has broadened and its scale length has increased by a factor of 8, the ion temperature scale length, L_{Ti} actually decreases 35%. The power balance analysis for this perturbation experiment indicates that the ion heat flux remains approximately constant throughout the perturbation, and is lower than theoretically predicted by fluid models. Consequently, the supershot transport does not adhere to marginal stability with regard to ITGDT. However, because of the observed $T_i > 2T_e$ and the presence of a substantial population of energetic particles in the plasma core, ITGDT-driven transport may not be so virulent as to impose marginal stability. This may be due to the linear and nonlinear Landau damping associated with the presence of hot and energetic ions.

IV. FAST-ION TRANSPORT

A number of measurements of fast-ion radial diffusion have been conducted on TFTR. Previous measurements of charge-exchange flux during off-axis neutral beam injection reported a fast-ion diffusivity less than 0.1 m^2/sec.[7,35] There have also been ongoing measurements of triton burnup[13,36,37] and escaping tritons[38,39] that require fast-triton diffusivity $\leqslant 0.1$ m^2/sec. Recently, fast-ion transport coefficients were modeled from the decay of neutron and charge-exchange flux decay following a fast-ion perturbation created with a short pulse (0.02 sec) of neutral beam power applied to an Ohmic plasma.[14] The neutron and charge-exchange flux measurements were modeled with both a Fokker–Planck calculation and a Monte Carlo calculation in the 1 1/2 D transport code TRANSP,[40] which includes collisional drag, energy diffusion, pitch angle scattering, neutral beam charge-exchange recapture, and a neutral density profile model. The neutron decay rate is classical, and is consistent with the fast ions having a diffusivity in the core of much less than 0.1 m^2/sec for these Ohmic discharges. Similarly, the charge-exchange flux measurement is modeled, and is consistent with either trapped particles, or fast ions at large radii, having a fast ion diffusivity of ~ 0.1 m^2/sec. These fast-ion diffusivities are small when compared to the ~ 1 m^2/sec obtained in perturbation experiments for helium ions and for electrons at thermal energies. There is now a few experimental data showing that transport of energetic particles is much slower than thermal particles.

V. DISCUSSION AND CONCLUSIONS

The combined application of steady-state and perturbative transport analysis techniques provides a powerful means of studying tokamak plasma transport. The diverse plasma regimes reviewed here can be summarized in the plot of diffusivity as a function of temperature (Fig. 9).[14] Several results obtained from steady-state and perturbative transport techniques are consistent with anomalous transport due to electrostatic drift-like microinstabilities. For the L-mode plasmas, the degradation of confinement with beam power is consistent with a strong temperature scaling. The helium particle diffusivity is observed to be on the order of χ_i, and the electron particle diffusivity is on the order of χ_e. Last, there is a rough correlation of density fluctuations with the thermal diffusivity in a neutral beam heating power scan. Although these general theoretical characteristics have been observed in the transport data, many details of the theory remain to be tested. The biggest problem is demonstrating that microinstability theory can match the amplitude and profile shape of the experimental transport coefficients.

In the case of the supershots, both steady-state and perturbative transport techniques show an improvement of core confinement. The reduced transport coefficients are correleated with density profile peakedness, but is not clear whether the peakedness causes the reduced transport. Other parameters, such as T_i/T_e and β_p, also correlate[28] and may

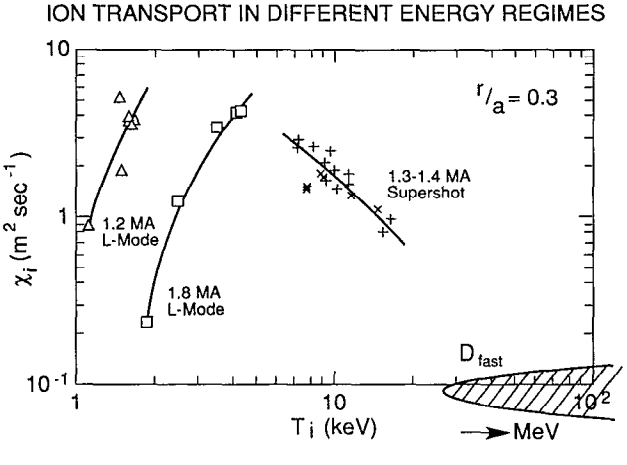

FIG. 9. Diffusivity versus temperature for L-mode plasmas, supershot plasmas, and fast ions.

be responsible for the changes in transport. The observed reversal of the temperature dependence of the diffusivity at high thermal temperature may also be related to the small values of diffusivity obtained for fast ions. With regard to the ITGDT mode, a perturbative experiment designed to test whether supershots are governed by marginal stability did not observe marginal stabilization or increased transport when the theoretical condition for mode instability was greatly exceeded. The experiments to test marginal stability perturbed the density gradients and temperature, and it will be necessary to design experiments that measure the scale length dependence in L mode to determine the type of drift-like microturbulence theory that is consistent with the transport.

Finally, energetic ion diffusion in many experiments is observed to be very small when compared to electron and ion thermal and particle transport coefficients. The fast-ion transport may be consistent with ion orbit averaging of electrostatic microinstabilities.[7,41] Most comparisons with theory crudely test the order of magnitude of the transport. Future work will need to examine the dependencies of fast-ion transport and make careful comparisons with detailed theories.

ACKNOWLEDGMENTS

We wish to acknowledge the physicists, engineers, technicians, and other staff members who support the TFTR program. We would like to acknowledge helpful discussions with J. Callen, and many of the participants in the Transport Task Force.

This work was supported by U.S. Department of Energy Contract No. De-AC02-76-CHO-3073.

[1] S. A. Cohen, J. L. Cecchi, and E. S. Marmar, Phys. Rev. Lett. **35**, 1507 (1975).
[2] J. D. Strachan, N. Bretz, E. Mazzucato, C. W. Barnes, D. Boyd, S. A. Cohen, J. Hovey, R. Kaita, S. S. Medley, G. Schmidt, G. Tait, and D. Voss, Nucl. Fusion **22**, 1145 (1982).
[3] N. L. Vasin, V. A. Vershkov, and V. A. Zhuraviev, Sov. J. Plasma Phys. **10**, 525 (1984).
[4] R. J. Fonck and R. A. Hulse, Phys. Rev. Lett. **52**, 530 (1984).
[5] R. C. Isler, Phys. Rev. Lett. **55**, 2413 (1985).
[6] K. W. Gentle, B. Richards, and F. Waelbroeck, Plasma Phys. Controlled Fusion **29**, 1077 (1987).
[7] P. C. Efthimion, M. Bitter, E. D. Fredrickson, R. J. Goldston, G. W. Hammett, K. W. Hill, H. Hsuan, R. A. Hulse, R. Kaita, D. K. Mansfield, D. C. McCune, K. M. McGuire, S. S. Medley, D. Mueller, A. T. Ramsey, S. D. Scott, B. C. Stratton, K.-L. Wong, TFTR Group, H. Biglari, P. H. Diamond, Y. Takase, and V. A. Vershkov, in *Plasma Physics and Controlled Nuclear Fusion Research 1988* Nice, France (IAEA, Vienna, 1989), Vol. 1, pp. 307–321.
[8] R. J. Goldston, Plasma Phys. Controlled Fusion **26**, 87 (1984).
[9] S. M. Kaye, Phys. Fluids **28**, 2327 (1985).
[10] M. Murakami, R. Isler, J. Lyon, C. Bush, L. Berry, J. Dunlap, G. Dyer, P. Edmonds, P. King, and D. McNeill, Phys. Rev. Lett. **39**, 615 (1977).
[11] K. H. Burrell, R. Stambaugh, T. Angel, C. Armentrout, F. Blau, G. Bramson, N. Brooks, R. Callis, R. Chase, A. Colleraine, J. DeBoo, D. Eames, S. Ejima, E. Fairbanks, J. Fasolo, R. Fisher, R. Freeman, J. Gilleland, R. Groebner, R. Harvey, C. Hsieh, R. Hong, G. Jahns, J. Kamperschroer, J. Kim, A. Lieber, J. Lohr, J. Luxon, M. Mahdavi, F. Marcus, D. McColl, T. McMahon, T. Ohkawa, N. Ohyabu, D. Overski, P. Petersen, T. Petrie, W. Pfieffer, J. Rawls, L. Rottler, J. Scoville, R. Seraydarian, R. Silagi, J. Smith, R. Snider, R. Stav, T. Taylor, T. Todd, J. Tooker, J. Treglio, D. Vaslow, J. Wesley, S. Wojtowicz, S. Wong, and G. Zawadzki, Nucl. Fusion **23**, 536 (1983).
[12] T. C. Luce, R. James, A. Fyareddinov, B. DeGentile, G. Giruzzi, Y. Gorelov, J. DeHaas, R. Harvey, S. Janz, J. Lohr, K. Matsuda, C. Moeller, T. Okazaki, C. Petty, R. Prater, L. Rodriguez, M. Saigusa, R. Snider, B. Stallard, and V. Trukhin, in *Plasma Physics and Controlled Nuclear Fusion Research 1990,* Washington, DC (IAEA, Vienna, in press).
[13] J. Strachan, M. Bitter, A. Ramsey, M. Zarnstorff, V. Arunasalam, M. Bell, N. Bretz, R. Budny, C. Bush, S. Davis, H. Dylla, P. Efthimion, R. Fonck, E. Fredrickson, H. Furth, R. Goldston, L. Grisham, B. Grek, R. Hawryluk, W. Heidbrink, H. Hendel, K. Hill, H. Hsuan, K. Jaehnig, D. Jassby, F. Jobes, D. Johnson, L. Johnson, R. Kaita, J. Kampershroer, R. Knoze, T. Kozub, H. Kugel, B. LeBlanc, F. Levinton, P. LaMarche, D. Manos, D. Mansfield, K. McGuire, D. McNeill, D. Meade, S. Medley, W. Schilling, G. Schmidt, S. Scott, S. Sesnic, J. Sinnis, F. Stauffer, B. Stratton, G. Tait, G. Taylor, H. Towner, M. Ulrickson, S. von Goeler, R. Wieland, M. Williams, K.-L. Wong, S. Yoshikawa, K. Young, and S. Zweben, Phys. Rev. Lett. **58**, 1004 (1987).
[14] S. Scott, C. Barnes, L. Grisham, G. Hammett, W. Heidbrink, D. Johnson, Y. Kusamsa, M. Zarnstorff, S. Zweben, M. Bell, M. Bitter, R. Boivin, R. Budny, C. Bush, A. Cavallo, C. Cheng, V. Decaux, P. Efthimion, R. Fonck, E. Fredrickson, R. Goldston, B. Grek, R. Hawryluk, K. Hill, H. Hsuan, R. A. Hulse, A. Janos, D. Jassby, F. Jobes, L. Johnson, R. Kaita, S. Kaye, P. LaMarche, D. Mansfield, J. McCauley, M. McCune, K. McGuire, S. Medley, D. Mueller, J. Murphy, H. Mynick, D. Owens, H. Park, R. Perkins, S. Pitcher, A. Ramsey, A. Roquemore, P. Rutherford, J. Schivell, G. Schmidt, B. Stratton, W. Stodiek, E. Synakowski, W. Tang, G. Taylor, H. Towner, S. vonGoeler, R. Waltz, R. Wieland, M. Williams, and K. Young, in *Plasma Physics and Controlled Nuclear Fusion Research 1990,* Washington, DC (IAEA, Vienna, in press).
[15] M. Zarnstorff, M. Bell, M. Bitter, C. Bush, R. Fonck, R. Goldston, B. Grek, R. Hawryluk, K. Hill, B. Howell, K. Jaehnig, D. Johnson, R. Knize, K. McGuire, A. Ramsey, G. Schilling, J. Schivell, S. Scott, and G. Taylor, in *Proceedings of the 15th European Conference on Controlled Fusion and Plasma Physics,* Dubrovnik, 1988 (European Physical Society, Petit-Lancy, Switzerland, 1988), Vol. 1, p. 95.
[16] D. W. Johnson, S. Scott, C. Barnes, M. Bell, M. Bitter, C. Bush, E. Fredrickson, B. Grek, K. Hill, H. Hsuan, D. Mansfield, H. Park, A. Ramsey, B. Stratton, E. Synakowski, G. Taylor, E. Towner, R. Weiland, and M. Zarnstorff, in *Proceedings of the 17th European Conference on Controlled Fusion and Plasma Physics,* Amsterdam, 1990 (European Physical Society, Petit-Lancy, Switzerland, 1990), Vol. 1, p. 114.
[17] P. C. Efthimion, D. K. Mansfield, B. C. Stratton, E. Synakowski, A. Bhattacharjee, H. Biglari, P. H. Diamond, R. J. Goldston, C. C. Hegna, D. McCune, G. Rewoldt, S. Scott, W. M. Tang, G. Taylor, R. E. Waltz, R. M. Wieland, and M. C. Zarnstorff, Phys. Rev. Lett. **66**, 421 (1991).
[18] B. B. Kadomtsev and O. P. Pogutse, Rev. Plasma Phys. **5**, 249 (1970).
[19] J. C. Adam, W. M. Tang, and P. H. Rutherford, Phys. Fluids **19**, 561 (1976).
[20] P. W. Terry, J. N. Leboeuf, P. H. Diamond, D. R. Thayer, J. E. Sedlak, and G. S. Lee, Phys. Fluids **31**, 2920 (1988).
[21] R. E. Waltz and R. R. Dominguez, Phys. Fluids B **1**, 1935 (1989).
[22] G. Rewoldt and W. M. Tang, Phys. Fluids B **2**, 318 (1990).
[23] N. L. Bretz, R. Nazikian, K. L. Wong, in *Proceedings of the 17th European Conference on Controlled Fusion and Plasma Physics,* Amsterdam, 1990 (European Physical Society, Petit-Lancy, Switzerland, 1990), Vol. 4, p. 1544.
[24] E. J. Synakowski, B. C. Stratton, P. C. Efthimion, R. J. Fonck, R. A. Hulse, D. W. Johnson, D. K. Mansfield, H. Park, S. D. Scott, and G. Taylor, Phys. Rev. Lett. **65**, 2255 (1990).
[25] R. A. Hulse, Nucl. Technol. Fusion **3**, 259 (1985).
[26] B. C. Stratton, E. J. Synakowski, P. C. Efthimion, R. J. Fonck, K. W. Hill, R. A. Hulse, D. W. Johnson, H. Park, G. Taylor, and J. Timberlake, Nucl. Fusion **31**, 171 (1991).
[27] R. Hawryluk, V. Aruanasalam, M. Bell, M. Bitter, W. Blanchard, N. Bretz, R. Budny, C. Bush, J. Callen, S. Cohen, S. Combs, S. Davis, D. Dimock, H. Dylla, P. Efthimion, L. Emerson, A. England, H. Eubank, R. Fonck, E. Fredrickson, H. Furth, G. Gammel, R. Goldston, B. Grek, L. Grisham, G. Hammett, W. Heidbrink, H. Hendel, K. Hill, E. Hinnov, S. Hiroe, H. Hsuan, R. Hulse, K. Jaehnig, D. Jassby, F. Jobes, D. Johnson, L. Johnson, R. Kaita, R. Kampershroer, S. Kaye, S. Killpatrick, R. Knize, H. Kugel, P. LaMarche, B. LeBlanc, R. Little, C. Ma, D. Manos, D. Mansfield, R. McCann, M. McCarthy, M. McCune, K. McGuire, D. McNeill, D. Meade, S. Medley, D. Mikkelsen, S. Milora, W. Morris, D. Mueller, V. Mukhovatov, E. Neischmidt, J. O'Rourke, D. Owens, H. Park, N. Pomphrey, B. Prichard, A. Ramsey, M. Redi, A. Roquemore, P.

Rutherford, N. Sauthoff, G. Schilling, J. Schivell, G. Schmidt, S. Scott, S. Sesnic, J. Sinnis, F. Stauffer, B. Stratton, G. Tait, G. Taylor, J. Timerlake, H. Towner, M. Ulrickson, V. Vershkov, S. vonGoeler, F. Wagner, R. Wieland, J. Wilgen, M. Williams, K.-L. Wong, S. Yoshikawa, R. Yoshino, K. Young, M. Zarnstorff, V. Zaveryaev, and S. Zweben, in *Plasma Physics and Controlled Nuclear Fusion Research 1986* (IAEA, Vienna, 1987), Vol. 1, p. 51.

[28] M. C. Zarnstorff, V. Aruanasalam, M. Bell, C. Barnes, M. Bitter, H.-S. Bosch, N. Bretz, R. Budny, C. Bush, A. Cavallo, T. Chu, S. Cohen, P. Colestock, S. Davis, D. Dimock, H. Dylla, P. Efthimion, A. Erhrardt, R. Fonck, E. Fredrickson, H. Furth, G. Gammel, R. Goldston, G. Greene, B. Grek, L. Grisham, G. Hammett, R. Hawryluk, H. Hendel, K. Hill, E. Hinnov, J. Hosea, R. B. Howell, H. Hsuan, R. A. Hulse, K. Jaehnig, A. Janos, D. Jassby, F. Jobes, D. Johnson, L. Johnson, R. Kaita, C. Kieras-Phillips, S. Killpatrick, V. Krupin, P. LaMarche, B. LeBlanc, R. Little, A. Lysoyvan, D. Manos, D. Mansfield, E. Mazzucato, R. McCann, M. McCarthy, M. McCune, K. McGuire, D. McNeill, D. Meade, S. Medley, D. Mikkelsen, R. Motley, D. Mueller, Y. Murakami, J. Murphy, E. Neischmidt, D. Owens, H. Park, A. Ramsey, M. Redi, A. Roquemore, P. Rutherford, T. Saito, N. Sauthoff, G. Schilling, J. Schivell, G. Schmidt, S. Scott, J. Sinnis, J. Stevens, W. Stodiek, J. Strachan, B. Stratton, G. Tait, G. Taylor, J. Timerlake, H. Towner, M. Ulrickson, S. vonGoeler, R. Wieland, M. Williams, J. Wilson, K.-L. Wong, S. Yoshikawa, K. Young, and S. Zweben, in *Plasma Physics and Controlled Nuclear Fusion Research 1988* (IAEA, Vienna, 1989), Vol. 1, p. 183.

[29] D. Jassby, C. Barnes, M. Bell, M. Bitter, R. Boivin, N. Bretz, R. Budny, C. Bush, H. Dylla, P. Efthimion, E. Fredrickson, R. Hawryluk, K. Hill, J. Hosea, H. Hsuan, A. Janos, F. Jobes, D. Johnson, L. Johnson, J. Kamperschroer, C. Kieras-Phillips, S. Killpatrick, P. LaMarche, B. LeBlanc, D. Mansfield, E. Marmar, M. McCune, K. McGuire, D. Meade, S. Medley, D. Mikkelsen, D. Mueller, D. Owens, H. Park, S. Paul, S. Pitcher, A. Ramsey, S. Sabbagh, S. Scott, J. Snipes, J. Stevens, J. Strachan, B. Stratton, E. Synakowski, G. Taylor, J. Terry, J. Timerlake, H. Towner, M. Ulrickson, S. vonGoeler, R. Wieland, M. Williams, J. Wilson, K.-L. Wong, K. Young, M. Zarnstorff, and S. Zweben, Phys. Fluids B **3**, 2308 (1991).

[30] S. Scott, V. Aruanasalam, C. Barnes, M. Bell, M. Bitter, R. Boivin, N. Bretz, R. Budny, C. Bush, A. Cavallo, T. Chu, S. Cohen, P. Colestock, S. Davis, D. Dimock, H. Dylla, P. Efthimion, A. Erhrardt, R. Fonck, E. Fredrickson, H. Furth, R. Goldston, G. Greene, B. Grek, L. Grisham, G. Hammett, R. Hawryluk, H. Hendel, K. Hill, E. Hinnov, D. J. Hoffman, J. Hosea, R. Howell, H. Hsuan, R. Hulse, K. Jaehnig, A. Janos, D. Jassby, F. Jobes, D. Johnson, L. Johnson, R. Kaita, C. Kieras-Phillips, S. Killpatrick, P. LaMarche, B. LeBlanc, R. Little, D. Manos, D. Mansfield, E. Mazzucato, M. McCarthy, M. McCune, K. McGuire, D. McNeill, D. Meade, S. Medley, D. Mikkelsen, R. Motley, D. Mueller, Y. Murakami, J. Murphy, Y. Nagayama, R. Nazakian, D. Owens, H. Park, A. Ramsey, M. Redi, A. Roquemore, P. Rutherford, G. Schilling, J. Schivell, G. Schmidt, J. Stevens, W. Stodiek, B. Stratton, E. Synakowski, W. Tang, G. Taylor, J. Timerlake, H. Towner, M. Ulrickson, S. vonGoeler, R. Wieland, M. Williams, J. Wilson, K.-L. Wong, S. Yoshikawa, K. Young, and S. Zweben, Phys. Fluids B **2**, 1300 (1990).

[31] M. C. Zarnstorff, C. Barnes, P. Efthimion, G. Hammett, W. Horton, R. Hulse, D. Mansfield, E. Marmar, K. McGuire, G. Rewoldt, B. Stratton, E. Synakowski, W. Tang, J. Terry, X. Xu, M. Bell, M. Bitter, N. Bretz, R. Budny, C. Bush, R. Fonck, E. Fredrickson, H. Furth, R. Goldston, B. Grek, R. Hawryluk, K. Hill, H. Hsuan, R. A. Hulse, D. Johnson, M. McCune, D. Meade, D. Mueller, D. Owens, H. Park, A. Ramsey, M. Rosenbluth, J. Schivell, G. Schmidt, S. Scott, G. Taylor, and R. Wieland, in *Plasma Physics and Controlled Nuclear Fusion Research 1990,* Washington, DC (IAEA, Vienna, in press).

[32] F. Romanelli, Phys. Fluids B **1**, 1018 (1989).

[33] T. Hahm and W. Tang, Phys. Fluids B **1**, 1185 (1989).

[34] N. Mattor and P. Diamond, Phys. Fluids B **1**, 1980 (1989).

[35] R. Radeztsky, S. Scott, R. Kaita, R. Goldston, G. Hammett, E. Fredrickson, S. Medley, R. Fonck, K. Hill, A. Ramsey, A. Roquemore, and M. Zarnstorff, in *Proceedings of the 15th European Conference Controlled Fusion and Plasma Physics,* Dubrovnik (European Physical Society, Petit-Lancy, Switzerland, 1988), p. 79.

[36] C. W. Barnes, H. Bosch, E. Nieschmidt, T. Saito, M. Bitter, A. Cavallo, P. Efthimion, B. Grek, W. Heidbrink, H. Hendel, K. Hill, H. Hsuan, D. Jassby, D. Johnson, L. Johnson, D. Mansfield, D. McCune, T. Murphy, H. Park, A. Ramsey, F. Stauffer, J. Stevens, J. Strachan, G. Tait, G. Taylor, H. Towner, K. Young, and M. Zarnstorff, in *Proceedings of the 15th European Conference on Controlled Fusion and Plasma Physics,* Dubrovnik (European Physical Society, Petit-Lancy, Switzerland, 1988), p. 87.

[37] P. Batistoni and C. W. Barnes, to appear in Plasma Phys. Controlled Nucl. Fusion.

[38] S. Zweben, R. Boivin, M. Diesso, S. Hayes, H. Hendel, H. Park, and J. Strachan, Nucl. Fusion **30**, 1551 (1990).

[39] S. Zweben, R. Boivin, R. Duvall, E. Fredrickson, R. Goldston, H. Mynick, J. Strachan, and R. White, Phys. Fluids B **2**, 1411 (1990).

[40] R. Hawryluk, in *Physics of Plasmas Close to Thermonuclear Conditions* (CEC, Brussels, 1980), Vol. 1, p. 65.

[41] H. Mynick and R. Duvall, Phys. Fluids B **1**, 750 (1989).